REPORT DOCUMENTATION PAGE

Form Approved
OMB NO. 0704-0188

1. AGENCY USE ONLY (Leave Blank)	2. REPORT DATE	3. REPORT TYPE AND DATES COVERED
		Reprint

4. TITLE AND SUBTITLE

Modeling viscoelastic properties of triblock copolymers: A DPD simulation study

5. FUNDING NUMBERS

W911NF-07-1-0268

6. AUTHOR(S)

Yelena R. Sliozberg, Jan W. Andzelm, John K. Brennan, Mark R. Vanlandingham, Victor Pryamitsyn, Venkat Ganesan

7. PERFORMING ORGANIZATION NAME(S) AND ADDRESS(ES)

University of Texas at Austin, Austin, Texas 78712, USA

8. PERFORMING ORGANIZATION REPORT NUMBER

9. SPONSORING / MONITORING AGENCY NAME(S) AND ADDRESS(ES)

U. S. Army Research Office
P.O. Box 12211
Research Triangle Park, NC 27709-2211

10. SPONSORING / MONITORING AGENCY REPORT NUMBER

11. SUPPLEMENTARY NOTES

The views, opinions and/or findings contained in this report are those of the author(s) and should not be construed as an official Department of the Army position, policy or decision, unless so designated by other documentation.

12 a. DISTRIBUTION / AVAILABILITY STATEMENT

Approved for public release;federal purpose rights

12 b. DISTRIBUTION CODE

13. ABSTRACT (Maximum 200 words)

Gel systems based on self-assembled, amphiphilic ABA triblock copolymers in midblock-selective solvent form stable, spatially extended networks with controllable morphology and tunable viscoelastic behavior. In this work, we systematically evaluate the mechanical properties of these gels using morphology calculations, and a nonequilibrium oscillatory shear technique based on the dissipative particle dynamics (DPD) method. Our simulations demonstrate that low molecular weight triblock copolymers with incompatible blocks self-assemble into micelles connected with bridges and loop-like chains comprised of the solvent-selective polymer midblocks. The fraction of bridges, b, generally increases with increasing relative volume of the midblock, x, defined as the ratio of midblock and endblock volumes (). For our model, b reaches a plateau at approximately $x > 9$ for a strongly selective solvent. At this limit, the value of b increases from 0.40 to about 0.66 as the copolymer concentration, c, increases from 0.2 to 0.5; however, this increase is less significant at higher concentrations. The elastic response of the gel studied here is comparable with the Rouse modulus. The elastic modulus increases with polymer concentration, and it exhibits a broad peak within $6 < x < 12$. Finally, we present an approximate method to predict the elastic modulus of unentangled ABA triblock copolymers based solely on the morphology of the micellar gel, which can be gleaned from equilibrium DPD simulations. We demonstrate that our simulation results are in good qualitative agreement with other theoretical predictions and experimental data.

14. SUBJECT TERMS	15. NUMBER OF PAGES
block copolymers ;DPD simulation ; gels morphology ; viscoelastic properties	12
	16. PRICE CODE

17. SECURITY CLASSIFICATION OR REPORT	18. SECURITY CLASSIFICATION ON THIS PAGE	19. SECURITY CLASSIFICATION OF ABSTRACT	20. LIMITATION OF ABSTRACT
UNCLASSIFIED	UNCLASSIFIED	UNCLASSIFIED	UU

NSN 7540-01-280-5500

Standard Form 298 (Rev.2-89)
Prescribed by ANSI Std. 239-18
298-102

Enclosure 1

Modeling Viscoelastic Properties of Triblock Copolymers: A DPD Simulation Study

YELENA R. SLIOZBERG,[1] JAN W. ANDZELM,[1] JOHN K. BRENNAN,[2] MARK R. VANLANDINGHAM,[1] VICTOR PRYAMITSYN,[3] VENKAT GANESAN[3]

[1]RDRL-WMM-A, U. S. Army Research Laboratory, Aberdeen Proving Ground, Maryland 21005-5069

[2]RDRL-WMB-D, U. S. Army Research Laboratory, Aberdeen Proving Ground, Maryland 21005-5069

[3]Department of Chemical Engineering, University of Texas at Austin, Austin, Texas 78712

Received 29 April 2009; revised 26 August 2009; accepted 26 August 2009
DOI: 10.1002/polb.21839
Published online in Wiley InterScience (www.interscience.wiley.com).

ABSTRACT: Gel systems based on self-assembled, amphiphilic ABA triblock copolymers in midblock-selective solvent form stable, spatially extended networks with controllable morphology and tunable viscoelastic behavior. In this work, we systematically evaluate the mechanical properties of these gels using morphology calculations, and a nonequilibrium oscillatory shear technique based on the dissipative particle dynamics (DPD) method. Our simulations demonstrate that low molecular weight triblock copolymers with incompatible blocks self-assemble into micelles connected with bridges and loop-like chains comprised of the solvent-selective polymer midblocks. The fraction of bridges, ϕ_b, generally increases with increasing relative volume of the midblock, x, defined as the ratio of midblock and endblock volumes ($x = \frac{V_B}{V_A}$). For our model, ϕ_b reaches a plateau at approximately $x > 9$ for a strongly selective solvent. At this limit, the value of ϕ_b increases from 0.40 to about 0.66 as the copolymer concentration, c, increases from 0.2 to 0.5; however, this increase is less significant at higher concentrations. The elastic response of the gel studied here is comparable with the Rouse modulus. The elastic modulus increases with polymer concentration, and it exhibits a broad peak within $6 < x < 12$. Finally, we present an approximate method to predict the elastic modulus of unentangled ABA triblock copolymers based solely on the morphology of the micellar gel, which can be gleaned from equilibrium DPD simulations. We demonstrate that our simulation results are in good qualitative agreement with other theoretical predictions and experimental data. © 2009 Wiley Periodicals, Inc.* J Polym Sci Part B: Polym Phys 48: 15–25, 2010

KEYWORDS: block copolymers; DPD simulation; gels; morphology; viscoelastic properties

INTRODUCTION Polymer gels based on blends of synthetic block copolymers in solvent exhibit thermal and environmental stability and possess controllable morphological and mechanical properties. Amphiphilic ABA triblock copolymers are one example of a polymer gel that has been widely used in many practical applications. ABA triblock copolymers undergo thermoreversible microphase separation in midblock-selective solvent and form spatially extended networks.[1,2] The microstructure of these gels depends on several factors such as temperature, copolymer concentration, block architecture, and relative size of the hydrophobic and hydrophilic blocks. The polymer networks that form consist of physical crosslinks comprising of solvent-incompatible endblocks (micelles) connected by the midblocks (bridges). The micelles are surrounded by a corona consisting of midblocks (loops), formed as a result of the close association of the endblocks. Some endblocks may not assemble into micelles, producing so-called tails and free-chains, where a tail has only one endblock associated with the network, whereas neither endblocks of a free-chain are part of the network. A schematic of such a polymer network is given in Figure 1. For unentangled triblock copolymers, the bridges can be considered as active chains of the network and are treated as elastic springs, whereas contributions to the gel network elasticity from loops, tails, and free-chains can be considered negligible.[3,4] For that reason, the bridge-to-loop ratio or bridge fraction is one of the key quantities that govern the mechanical properties of a gel. The bridge fraction depends on several factors, such as copolymer concentration, degree of block incompatibility, and the relative size of the blocks. Experimental observations have revealed that the bridge fraction increases with relative size of the midblock (with respect to the endblocks) and copolymer concentration.[5–7]

The network resulting from bridging strongly influences several mechanical properties that are often used to characterize the gels. For example, when a linear viscoelastic material is subjected to oscillatory strains, γ, of frequency, ω, the stress response, σ, is necessarily cyclic and can be written

Correspondence to: Y. R. Sliozberg (E-mail: yelena.r.sliozberg@arl.army.mil)
Journal of Polymer Science: Part B: Polymer Physics, Vol. 48, 15–25 (2010)

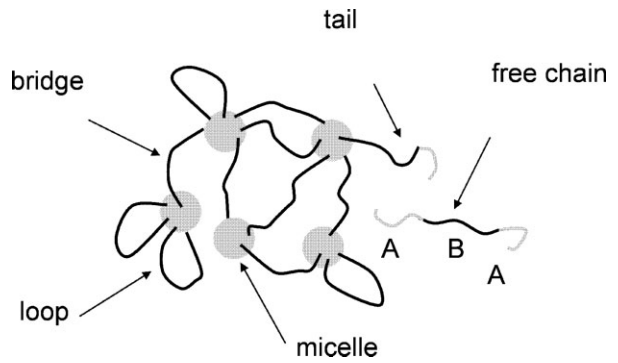

FIGURE 1 Schematic representation of a polymer network formed from an ABA triblock copolymer in a midblock-selective solvent.

as: $\sigma(\omega) = A_\omega\ (G'(\omega)\sin(\omega t) + G''(\omega)\cos(\omega t))$, where A_ω is the amplitude. The storage modulus, $G'(\omega)$, characterizes the material's ability to store energy, and the loss modulus, $G''(\omega)$, characterizes the amount of energy lost through viscous processes. For gels, $G'(\omega)$ often is only weakly dependent on ω over a broad range and is several orders of magnitude larger than $G''(\omega)$. Thus, a reasonable assumption is to define the elastic response of a gel by referring to the plateau value of G' or the equilibrium elastic modulus, G_e.[8] G_e for an ABA gel made from unentangled chains in the semidilute regime in a selective solvent is comparable with modulus of Gaussian network in a good solvent G_e,[8,9] expressed as

$$G_e^{\text{Rouse}} = RT\phi_b\left[\frac{C}{M_w}\right] \quad (1)$$

where C is a mass/volume concentration, M_w is the molar mass of the triblock copolymer, T is the temperature, R is the universal gas constant, and ϕ_b is the previously defined bridge fraction. For copolymers with higher molecular weight, entanglements would give rise to a large additional contribution to the elastic modulus, and the value of G_e would be an order of magnitude higher than that predicted with eq 1. According to classical polymer theory, G_e for entangled polymers is proportional to $1/N_e c^{2.3}$, where N_e is the number of concentration blobs per entanglement with size, $\xi = c^{-1(3\nu-1)}$, c is the volume fraction of polymer, and ν is the Flory exponent ($\nu = 0.588$).[10,11]

Several studies using molecular simulation have corroborated and expanded the theoretical picture of the morphology and mechanical properties of gels formed from ABA triblock copolymers in midblock-selective solvent.[12–16] Khalatur et al.[17,18] studied the micellar organization and rheology of the triblock gels and found that equilibrium microstructures of these gels depends on the chain rigidity, and that their rheological properties are governed by the spatial distribution of bridges between micelles.

Moreover, there have been several theoretical and computational efforts undertaken to gain a physical understanding of the role of the bridge fraction on the network. By using self-consistent field theory, Zhulina and Halperin[19] have demonstrated that the bridge fraction is proportional to the degree of incompatibility, $\phi_b \propto (\chi M)^{-1/9}$. Matsen and Schick[20] have shown that ϕ_b decreases slowly with increasing polymer length, M, increasing Flory-Huggins parameter, χ, and decreasing endblock fraction in the strongly segregated lamellar phase. Although Matsen and Schick found that the bridge fraction was typically equal to 0.40, Jones et al.[21] found the bridge fraction to be approximately equal to 0.63 for the strong segregation limit. An increase of ϕ_b with copolymer concentration has also been reported by Monte Carlo simulation studies,[4,22–24] where Karatasos et al.[23] estimated the bridge fraction to be in the range of 0.37–0.50, with increasing molecular weight of the triblock. Nguyen-Misra and Mattice have demonstrated that the bridge fraction increases with copolymer concentration and block incompatibility. The same authors observed that the bridge fraction was slightly higher with an increase of the relative midblock size, but found this increase to be insignificant.[24] These theoretical findings have been partially confirmed by experimental work.[7,25] Watanabe et al.[7] demonstrated that the bridge fraction increases from 0.2 to 0.4 with increasing copolymer concentration from 20 to 50 weight percent. Takano et al. obtained a bridge fraction equal to 0.93, which is higher than theoretical predictions and other experimental work. They attributed this finding to the possible existence of interlocked entanglements.[26]

Despite the significant impact that these computational and theoretical studies have made to our understanding of the structure and mechanical properties of triblock copolymers, there are some considerable shortcomings. Micellar phases are characterized by fluctuation effects; hence, they may not lend themselves to an accurate implementation of methods such as self-consistent field theories. Furthermore, the Monte Carlo approach does not lend itself to the simulation of the dynamics of fluids. Moreover, the impact of chemical and compositional variables on the bridge-to-loop ratio of triblock gels has yet to be systematically studied by a particle-based dynamics approach at either the molecular or mesoscale. To address this shortcoming, we present a dissipative particle dynamics (DPD) simulation study of the ABA triblock copolymer in a B-selective solvent. In this study, we attempt to create, through computational modeling, a predictive tool that answers questions regarding the impact of concentration and molecular architecture on the morphology, in particular the bridge fraction, and viscoelastic properties of ABA gels. Understanding such structure-property relationships will enable the development of thermoreversible gels with the desired morphological and mechanical properties that meet the specific application needs.

MODEL AND SIMULATION METHODS

Generally speaking, atomistic molecular dynamics is suitable up to 10 nm and several nanoseconds, making it difficult to perform simulations of large polymeric systems on comparable timescales. In this study, we have exploited the DPD simulation technique, consisting of coarse-grained particles that represent clusters of molecules rather than individual

atoms.[27,28] The DPD method is a mesoscale simulation technique that operates at time and length scales larger than those of traditional molecular dynamics, whereas providing the ability to probe phenomena that is inaccessible to continuum modeling.

Dissipative Particle Dynamics

A DPD system is composed of soft particles, each representing a region of fluid, moving according to Newton's equations of motion continuously in space and discreetly in time. In a DPD simulation of polymers, the chain is modeled as a collection of point particles that represent lumps of the chain containing several segments. DPD particles are defined by mass, m_i, position, r_i, and velocity, v_i, and interact with each other via a pairwise, two-body, short-ranged force, **F**, that is written as the sum of a conservative force, $\mathbf{F}^{C}$, dissipative force, $\mathbf{F}^{D}$, and random force, $\mathbf{F}^{R}$, as follows:

$$\mathbf{F}_i = \sum_{j\neq i} \mathbf{F}_{ij}^{C} + \sum_{j\neq i} \mathbf{F}_{ij}^{D} + \sum_{j\neq i} \mathbf{F}_{ij}^{R} \tag{2}$$

where $\mathbf{F}^{C}$ includes a soft repulsion force, $\mathbf{F}^{Cr}$, acting between two particles and a Finite Extensible Nonlinear Elastic (FENE) force, $\mathbf{F}^{FENE}$, acting between adjacent particles in a polymer chain. The DPD polymer chains defined in this manner are flexible, because no additional constraints, such as bond bending or bond torsion, are included. $\mathbf{F}^{Cr}$ and $\mathbf{F}^{FENE}$ are given by

$$\mathbf{F}_{ij}^{Cr} = \begin{cases} a_{ij}\left(1-\frac{r_{ij}}{r_c}\right)\mathbf{e}_{ij} & \text{for } r_{ij} < r_c \\ 0 & \text{for } r_{ij} \geq r_c \end{cases} \tag{3}$$

and

$$\mathbf{F}_{ij}^{FENE}(\mathbf{r}) = \frac{H}{1-\left(\frac{r_{ij}}{l}\right)^2}\mathbf{r}. \tag{4}$$

In eqs 3 and 4, a_{ij} is the maximum repulsion between particle i and particle j, $r_{ij} = |\mathbf{r}_i - \mathbf{r}_j|$, $\mathbf{e}_{ij} = (\mathbf{r}_i - \mathbf{r}_j)/r_{ij}$ is the unit vector from the *jth* particle to the *ith* particle, r_c is the cutoff radius, H is the spring constant, l represents the maximum extension length of a polymer bond, and **r** is the vector that connects pairs of adjacent particles in a polymer chain. The remaining two forces, $\mathbf{F}^{D}$ and $\mathbf{F}^{R}$, are given by

$$\mathbf{F}_{ij}^{D} = -\gamma\omega^{D}(r_{ij})(\mathbf{e}_{ij}\mathbf{v}_{ij})\mathbf{e}_{ij}, \tag{5}$$

and

$$\mathbf{F}_{ij}^{R} = \sigma\omega^{R}\frac{\xi_{ij}}{\sqrt{\Delta t}}\mathbf{e}_{ij}, \tag{6}$$

where $\omega^{D}(r)$ and $\omega^{R}(r)$ are weight functions, γ is the friction coefficient, σ is the noise amplitude, $\mathbf{v}_{ij} = \mathbf{v}_i - \mathbf{v}_j$, ξ_{ij} is the Gaussian random number with zero mean and unit variance that is chosen independently for each pair of interacting particles, and Δt is the time step.

Español and Warren[29] showed that the system samples the canonical ensemble and obeys the fluctuation-dissipation theorem (in the limit of $\Delta t \to 0$) if the following relations hold.

$$\omega^{D}(r) = \left[\omega^{R}(r)\right]^2, \tag{7}$$

and

$$\sigma^2 = 2\gamma k_B T, \tag{8}$$

where T is the temperature, and k_B is Boltzmann's constant. $\omega^{R}(r)$ is typically chosen[29] as

$$\omega^{R}(r) = \begin{cases} 1-\frac{r}{r_c} & \text{for } r < r_c \\ 0 & \text{for } r \geq r_c \end{cases}. \tag{9}$$

For a more detailed description of the DPD method, see the original articles by Hoogerbrugge and Koelman.[27,28]

Coarse-Grained Model of $A_1B_xA_1$ Triblock Copolymer

The three-dimensional system consists of a total of N_t DPD particles of triblock copolymers connected by a FENE force, plus solvent in a cubic domain with periodic boundaries in all directions. The system has N chains of an $A_1B_xA_1$ triblock copolymer comprised of particles of types "A" and "B" of total length M immersed in a midblock-selective solvent whose particles are of type "S." Each DPD particle represents roughly the same volume. Each chain has two endblocks represented by a single particle of type "A" and a midblock comprised of x particles of type "B." See Figure 2 for a schematic of an $A_1B_3A_1$ triblock copolymer.

The size of the DPD particle in the simulated chain should be larger than or equal to a Kuhn's segment of the polymer to ensure the flexibility of the polymer on the mesoscopic scale.[30]

The number of triblock chains is chosen from

$$N = \frac{cN_t}{M}, \tag{10}$$

where $M = x + 2$ and c is the volume fraction of the triblock in the solution, and x is the number of particles making up the midblock. The endblocks for all triblocks are modeled as a single particle to avoid any occurrence of the chain collapsing on itself before any association with other endblocks takes place.

The physical size of the interaction radius for the DPD particle, r_c, depends on the molar volume of the endblock[31] and may be estimated from

$$r_c = \sqrt[3]{\frac{\rho_{DPD} v_A}{N_A}}, \tag{11}$$

where $\rho_{DPD} = \frac{N_t}{V_t}$ is the DPD particle density, V_t is the total volume of the system, v_A is the molar volume of the endblock, and N_A is Avogadro's number. The number of midblock particles, x, is evaluated from the volume fraction of the endblock in the dry copolymer, f_A, written as

$$x = \frac{2(1-f_A)}{f_A}. \tag{12}$$

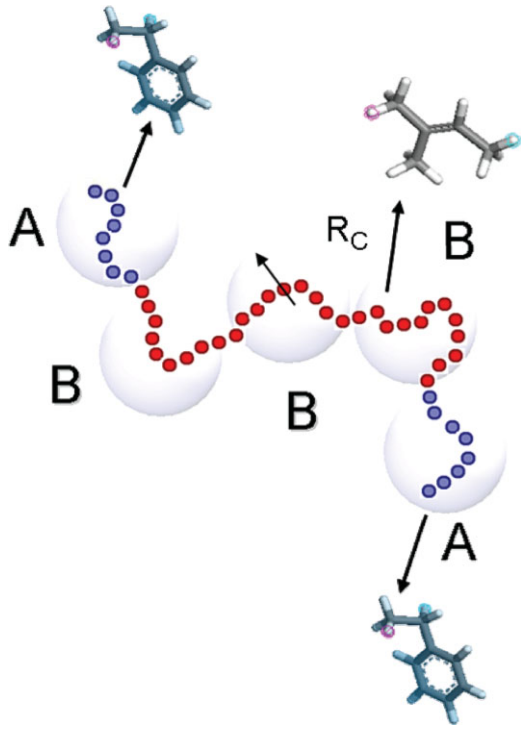

FIGURE 2 Schematic representation of an $A_1B_3A_1$ triblock copolymer mapped onto a DPD model. The poly(styrene-isoprene-styrene) copolymer is chosen as an example.

Note that because the endblock of any length is represented by one DPD particle, x corresponds to the relative volume of the midblock in the triblock copolymer: $x = V_B/V_A$, where V_A and V_B are volumes of the midblock and endblock, respectively.

Viscoelastic Property Calculations

Simulations have been used to determine the parameters that govern the viscoelastic behavior of polymer systems, delineating the regimes and frequencies at which various effects (e.g., polymer chain length) are manifested. Because of the soft nature of the DPD potentials used in this study, polymer chains can pass freely through each other, thus our simulations cannot mimic chain uncrossability.[32] The viscoelastic properties, such as storage, $G'(\omega)$, and loss moduli, $G''(\omega)$, can be calculated using a nonequilibrium oscillatory shear technique,[33,34] entailing a simulation with an additional force in the shear direction, along with time-dependent Lees-Edwards boundary conditions.[35] For oscillatory shear imposed in the x-y plane, the equation of motion for the particle velocities becomes[34]

$$m_i \frac{dv_{ix}}{dt} = F_{ix} + m_i r_{iy} \frac{d^2\gamma(t)}{dt^2}. \tag{13}$$

The oscillatory strain has been taken as $\gamma(t) = A_\omega \sin(\omega t)$, where A_ω and ω are values chosen for the amplitude and frequency, respectively. We have used $A_\omega = 0.1$ that corresponds to the linear rheology regime and an oscillation period, $p = 2\pi/\omega$ from 10^1 to 10^4.

The equilibrium DPD approach allows us to define the various conformations of the midblocks (bridges, loops, and dangling tails) and precisely calculate their quantities. Afterwards, we can correlate the structural properties of the triblock gel with the elastic modulus obtained from the oscillatory shear simulations.

Assuming that the crosslinks (micelles) are fixed and moving in an affine manner, the equilibrium elastic modulus, G_e, can be evaluatedas a sum of the contributions of the different conformations of the midblock,[7] as follows:

$$G_e = \nu_b G_b + \nu_l G_l + \nu_t G_t \tag{14}$$

where ρ is the copolymer density, ν_b, ν_l, and ν_t are the number densities of bridges, loops, and dangling tails, respectively, and where G_b, G_l, and G_t are the elastic modulus of a

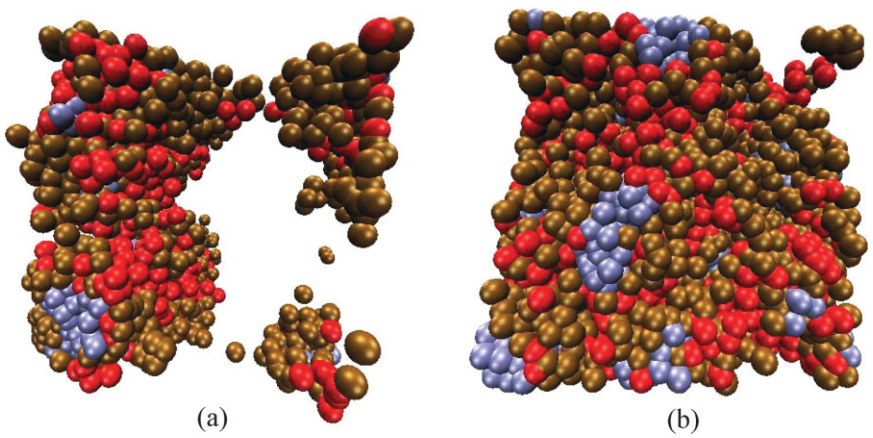

FIGURE 3 Snapshots from a DPD simulation of our model $A_1B_6A_1$ copolymer for the system size of 15000 DPD particles, where micelles comprised of type "A" particles are colored blue, and bridge and loop conformations of the midblocks of type "B" particles are colored red and brown, respectively. For visual clarity, solvent particles are not shown. The equilibrated structures are for (a) $c = 0.2$ and (b) $c = 0.4$.

TABLE 1 Repulsive Parameters Between a Pair of DPD Particles

DPD Pair	S-S	A-A	B-B	A-B	A-S	B-S
a_{ij}	50.0	50.0	50.0	66.0	105.0	50.0

single bridge, loop, or dangling tail, respectively. In the high-segregation regime, the number of tails is negligible and the midblocks adopt either a bridge or loop conformation. By using eq 10 and evaluating the number of bridges, $N_b = N\phi_b(x, c)$, and the number of loops, $N_l = N(1 - \varphi_b(x, c))$, we can determine the equilibrium elastic modulus in DPD units as:

$$G_e = \rho_{DPD}\frac{c}{x+2}[G_b\phi_b(x,c) + G_l(1-\phi_b(x,c))] \quad (15)$$

where $\phi_b(x, c)$ is the bridge fraction and is a function of the relative block size and copolymer concentration. With $\phi_b(x, c)$ and G_e evaluated from the equilibrium and oscillatory shear simulations, respectively, we can estimate the contributions of a single bridge or loop to the elastic modulus.

Simulation Parameters

DPD-reduced units are adopted for the convenient expression of parameters and are taken as length in r_c, energy in k_BT/r_c, mass in particle mass m, and time in $\tau = r_c\sqrt{m/k_BT}$.[31] Therefore, the actual value of the moduli are calculated from the moduli expressed in DPD units, G_{DPD} as

$$G = G_{DPD}k_BT/(r_c)^3 \quad (16)$$

We choose standard values of $m = k_BT = r_c = 1$, time step $\Delta t = 0.01$ and overall particle density $\rho_{DPD} = 3$. H and l in eq 4 for the triblock are 1 and 3, respectively, which gives the length of a single bead-spring unit equal to one Kuhn's segment, $b_{DPD} = \frac{3k_BT}{Hl} = 1$.[36]

We have chosen the repulsive parameter for like-particles, a_{ii}, for all types of particles to be equal to 50. Groot and Warren determined a_{ii} by matching the dimensionless compressibility for a real system, k^{-1}, and the DPD fluid according to the scaling rule $a_{ii} = k_BT\frac{k^{-1}N_m - 1}{2\alpha\rho_{DPD}}$, where N_m is the level of coarse-graining and α is determined to be 0.101 ± 0.001.[31,37] For water at $\rho_{DPD} = 3$, $k_BT = 1$ and under standard conditions ($k^{-1} = 15.98$), Trohimov estimated the maximum level of coarse-graining should be $N_m^{max} = 10$ water molecules to represent one DPD particle.[38] Having N_m larger than N_m^{max} would give $a_{ii} > 250$ and cause an artificial solidification of the liquid system.[38,39] Thus by modeling tens of polymer units as a single DPD particle, we are greatly exceeding the value of N_m^{max}. Conversely, Nakamura and Tamura[40] have shown that the dependence of the morphology of an A-B type chain in an A-selective solvent on a_{ii} is weaker than the dependence on a_{ij}. It is not always possible to correctly map an atomistic simulation to a mesoscale representation;[41] therefore, the choice of $a_{ii} = 50$ seems to be reasonable.

The repulsive parameters for unlike-particles a_{ij} are determined according to a linear relationship with the Flory-Huggins parameter[37]:

$$a_{ij} \approx a_{ii} + 3.27\chi_{ij}. \quad (17)$$

where χ_{ij} parameters are mapped from long polymers to the shorter DPD chains while preserving $\chi M = const$. We have chosen the excess repulsion $\Delta a = 3.27\chi_{ij}$ for an A-B pair equal to 55. This value corresponds to the strong segregation regime, $\chi M \approx 85 - 340$, where M changes from 5 to 20. Interaction parameters between blocks of the copolymer and solvent are chosen such that $\chi_{AS} \approx 5$ and $\chi_{BS} = 0$, respectively, to model a perfectly selective solvent, i.e., nonsolvent for the A-block and good solvent for the B-block.

The maximum repulsive force parameters used in this study are summarized in Table 1.

Methodology

This study investigates the role of the relative block size and triblock copolymer concentration on the structure and structure-related mechanical properties of the polymeric gels that form. To probe the effect of concentration and relative block size, we considered a range of values for both c (0.2, 0.3, 0.4, and 0.5) and x.[3,6,9,12,15,18]

Equilibrium configurations were generated by randomly placing polymer chains and solvent particles into the simulation box, followed by slowly adjusting the periodic box size to the desired pressure. This was followed by a constant temperature simulation for 1000 steps. An equilibrium state was determined by repeating this procedure six times until the system pressure was stable within 1%. Ten parallel simulations were run for each set of initial conditions to minimize statistical uncertainty. After equilibration of the structure, a series of stress trajectories was generated by imposing the oscillatory shear conditions with 0.1% strain. Because DPD simulations are generally able to access only frequencies in the megahertz regime, dynamic moduli were linearly extrapolated. Note that numerical errors tend to be higher at low frequencies requiring averaging over more stress trajectories to minimize these errors.

We examined the microstructure of each equilibrium state to determine the conformation of each midblock in the gel using the following scheme. First, we identified all crosslinks or micelles. A micelle was defined as two or more endblocks in close proximity, such that any two of these endblocks were separated by less than r_c. Next, we identified the conformation of the midblocks. The midblock was considered to be in a loop conformation if both endblocks belong to the same micelle, whereas if the midblock connected two different micelles, then it was considered to be in a bridge conformation. Finally, an unassociated endblock also was assumed to form a dangling tail conformation for the midblock.

To explore the system size effects, we performed equilibrium and nonequilibrium DPD simulations of the $A_1B_6A_1$ triblock copolymer in midblock selective solvent for various system sizes: 5000, 15,000, and 30,000 DPD particles, where results

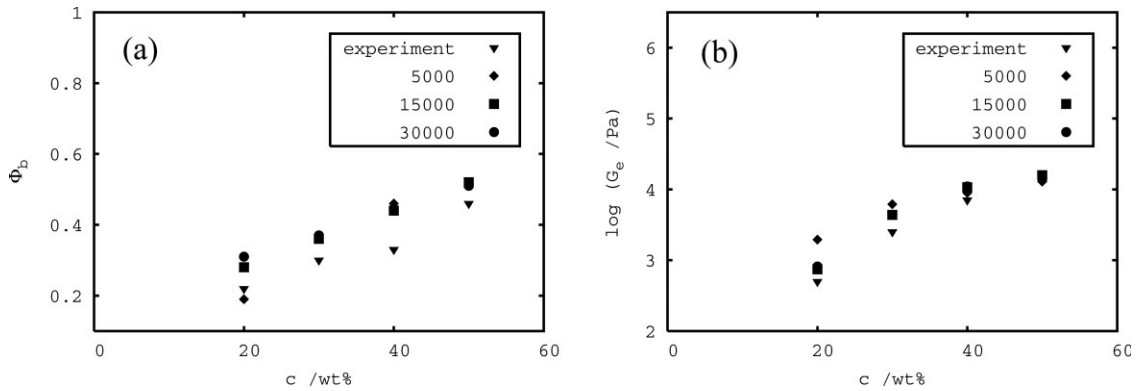

FIGURE 4 (a) Bridge fraction, ϕ_b and (b) equilibrium modulus, G_e as a function of copolymer concentration, c/wt % from the experimental measurements of the SIS system (7) and DPD simulations of the $A_1B_6A_1$ triblock copolymer copolymer for simulated system sizes of 5000, 15000, and 30000 DPD particles.

are presented in Figure 4. From Figure 4, it is clear that the bridge fraction and elastic modulus at $c > 0.2$ do not significantly depend on the system size (the error is within 4%), but the bridge fraction and elastic modulus at $c = 0.2$ are indeed strongly affected by the system size. The simulation results for 15,000 and 30,000 particles are similar for the entire concentration range. On the basis of these findings, we studied the morphology and rheology of the triblock copolymer in the midblock selective solvent at $c > 0.2$ for the entire range of midblock size with 5000 total number of DPD particles. For these simulations, we used a periodic box with dimensions $11.9 \times 11.9 \times 11.9$ (in reduced DPD units), which is more than $3\times$ larger than the maximum diameter of the micelles obtained from our simulation. Therefore, we do not expect any significant finite size effects. However, we carried out equilibrium and nonequilibrium simulations at $c = 0.2$ with a larger system of 15,000 DPD particles for the entire range of the midblock size. In addition, we have carried out an equilibrium DPD simulation of the $A_1B_{12}A_1$ triblock copolymer with 15000 DPD particles at various concentrations to study the effect of concentration and relative block size on the morphology of the system.

RESULTS AND DISCUSSION

Validation of Our Method

The poly(styrene-isoprene-styrene) block copolymer, or SIS, in an isoprene-selective solvent has been chosen as a model triblock copolymer for this study because of the sufficient amount of experimental structural and rheological data available.[1,2,7,25] To validate our method, we choose $A_1B_6A_1$ in a B-selective solvent as a prototype of the SIS copolymer in the I-selective solvent, *n*-tetradecane, studied by Watanabe et al.[7] Molecular weights for the *S*-endblock and the I-midblock are 7.2 kg/mol and 35.8 kg/mol, respectively. Dynamics measurements have shown from that the bead-spring model accurately describes polystyrene if it has a single bead-spring unit, *b* equal to 5.0 nm, corresponding to ~50 monomers.[42,43] By mapping ~70 monomers of the polystyrene block to a single DPD particle, we anticipate obtaining a reasonably accurate mesoscale representation of our system using a chain of 8 DPD particles.

At room temperature, the Flory-Huggins interaction parameter for the copolymer blocks $\chi_{PS\text{-}PI}$ has been estimated as 0.11[44] (which corresponds to $\chi M \approx 90$), whereas for the polystyrene block and *n*-tetradecane, $\chi_{PS\text{-}TETRA}$ has been estimated as 1.83.[45] These parameters are matched to our copolymer model in a strongly selective solvent with a large degree of incompatibility of the blocks.

We have studied the following weight-percent concentrations of $A_1B_6A_1$, 0.2, 0.3, 0.4, and 0.5, which correspond to volume fractions 0.17, 0.28, 0.39, and 0.50, respectively. The triblock is expected to adopt micellar morphology at room temperature for this concentration range. All simulation runs resulted in microphase separation, which led to a three-dimensional network structure of a micellar gel with the midblock exhibiting bridge or loop conformations. This finding is in agreement with the experimental study of Laurer et al.[1] For a similar system, SIS/mineral oil, they observed micellar morphology at a styrene concentration <0.2 weight-percent.[1] Figure 3 shows an example of an equilibrated system from our DPD simulations for $c = 0.2$ and $c = 0.4$. Figure 3(a) shows a separation of copolymer solution into densely packed micellar phase and "soft" (solvent) phase at $c = 0.2$. We will talk about this phenomenon in details in the latter sections.

Figure 4(a) compares the estimated loop fractions of the midblock from the DPD simulation with those obtained by Watanabe et al.[7] by measuring the dielectric losses of the SIS in *n*-tetradecane. Simulation results are in good qualitative agreement with the experimental data at all concentrations.

The storage modulus, G' obtained from our simulations has a numerical value close to a plateau for the frequencies accessible in a DPD simulation. (The loss modulus $G''(\omega)$ is not a point of interest in this study.) The equilibrium value of the storage modulus, G_e determined from our DPD simulations has been mapped back to its actual value using eq 16. Figure 4(b) shows the simulated and experimental rheological data and illustrates the relatively accuracy of the DPD model. The

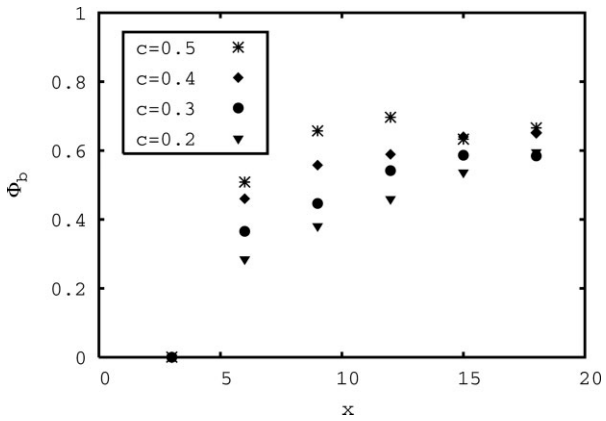

FIGURE 5 Bridge fraction, ϕ_b for $A_1B_xA_1$ copolymer as a function of the relative block size, x at various volume fractions of the triblock, c.

I-blocks in the SIS solutions are minimally entangled due to their low molecular weight ($M_w \approx 35000$), when compared with entanglement molecular weight, $M_e' = M_e/c$ with $M_e = 6200$ is entanglement molecular weight in the bulk.[46] Hence, DPD simulation results are expected to be in good agreement with the experimental data.

Bridge Fraction

To compare the effects of the concentration and relative block size on the equilibrium bridge fraction, ϕ_b, we have performed a set of equilibrium DPD simulations with variable concentration, c, and relative volume of the midblock, x, where results are presented in Figure 5. Our results indicate that ϕ_b increases with increasing copolymer concentration; however, increases of ϕ_b are somewhat less significant at higher concentrations. Likewise, we have found that ϕ_b increases with increasing relative volume of the midblock if the value of the midblock volume is of the order of magnitude of the endblock volume ($x < 9$). For the relatively large midblock compared with the endblock ($x \geq 9$), ϕ_b only weakly depends on x and reaches some constant value in the range of 0.40 to 0.66 depending on copolymer concentration. This behavior is a result of the reduction of the entropic penalty of stretching the bridging midblock. A decrease in the bridge stretching can be achieved either with decreasing of the average distance between the micelles as copolymer concentration increases,[24] or from an increase in the relative size of the midblock. When the concentration is sufficiently high, the distance between micelles becomes shorter; consequently, the effect of concentration on the bridge fraction is weaker. Decreasing the average spacing between micelles with increasing concentration has also been reported by Seitz et al.[47] Likewise, the effect of the relative block size on the bridge fraction becomes negligible when the midblock is sufficiently long, so that micelles bridge without significant stretching. The compact size of the midblock compared with the distance between micelles can also lead to the tendency to form loops for low x.[5] For example, for $x = 3$, all midblocks form loops for the entire concentration range. It is important to mention that ϕ_b does not depend on the absolute volume of the blocks but rather depends on the relative block sizes.

For a relatively high degree of incompatibility and strongly selective solvent conditions, ϕ_b is only a function of concentration and the triblock architecture. However, in general, ϕ_b also depends on the degree of incompatibility and miscibility of the copolymer blocks and solvent, $\phi_b = f(c, x, \chi_{ij})$, where indices i and j represent A, B, and S particles. This dependence becomes significant for endblocks with a low degree of polymerization in a slightly selective solvent. For this case, some endblocks would not associate in micelles, producing dangling tails and subsequently decreasing both ϕ_b and ϕ_l.[24] To study this behavior, we could systematically vary the repulsive parameters in our model and then evaluate ϕ_b; however, we leave such a study for future work.

Although our simulation model allows reorganization of midblocks during the simulation, the bridge-to-loop ratio can be assumed constant for the length of our simulation runs. To verify, we have continued to run the $A_1B_{12}A_1$ system for another six simulation cycles (simulation time was 6000 in DPD units) and found that the average bridge fraction changed less than 1%. Also, we have checked the characteristic time of the bridge-to-loop transformation and found that it is a relatively long event, $\tau \sim 10^3$ in DPD units. Figure 6 shows the average exchange time of the midblock for the $A_1B_{12}A_1$ triblock copolymer. The loops become less stable as concentration increases. This finding is related to the entropic penalty associated with forcing both endblocks to reside in the same micelle.[47] Bridges are more short-lived at $c = 0.2$ as a result of stretching in the gel exhibiting syneresis. At $c > 0.2$, the bridge-to-loop exchange time does not depend on concentration.

Syneresis of ABA Gels

According to our simulation results, the micelles of ABA copolymers are typically formed at a distance comparable with the midblock size to avoid both bridge stretching. If the concentration of the chains is small and the midblock is relatively short, micelles tend to be crowded, and this

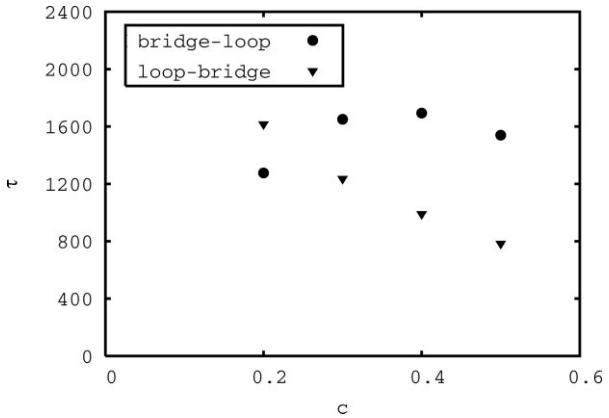

FIGURE 6 The characteristic time of the bridge-to-loop and loop-to-bridge exchange as a function of concentration for the $A_1B_{12}A_1$ copolymer.

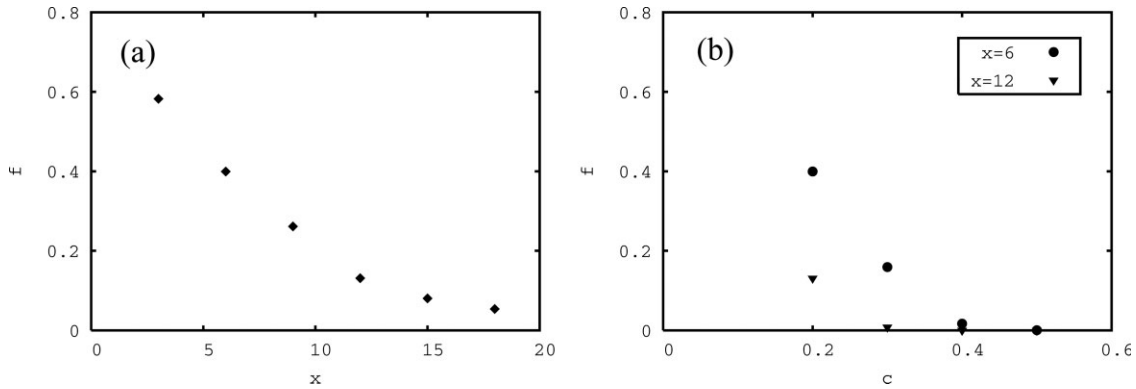

FIGURE 7 Volume fraction of the solvent phase, *f*, as a function of (a) the midblock size, *x* at $c = 0.2$ and (b) copolymer 3concentration, *c* for the $A_1B_6A_1$ and $A_1B_{12}A_1$ copolymers.

occurrence consequently results in syneresis wherein separation of the polymer solution into two macrophases, i.e., a densely packed micelle phase and a solvent-rich phase.[11,48] Figure 3(a) shows an example of a gel exhibiting syneresis with a distinct "soft" region (solvent phase) in a copolymer solution at low *c*. We have probed an extent of syneresis by measuring the volume fraction of the solvent phase, f and defined it as $f = \frac{V_{\text{free}}}{V_t}$, where V_{free} and V_t are volume of solvent phase and total volume of the system, respectively. We have partitioned our simulation box into bins, where the bin size is approximately equal to the average size of the micelles. Then, we computed the number of the bins occupied by pure solvent, n_0. We have evaluated f from $f = n_0 V_{\text{bin}}$, where V_{bin} is the volume of the bin. We have presented our results in Figure 7. Our simulations have shown that f increases with decreasing concentration and block size. For the copolymer with a small midblock, the syneresis occurs even for higher concentration, for example for the $A_1B_6A_1$ triblock at $c = 0.3$.

On the basis of the observation of the system undergoing syneresis, we expect to find the elastic modulus lower at $c = 0.2$ than the one estimated from morphology calculations. We will discuss this feature in the latter section.

Elastic Shear Modulus

To assess the effect of concentration and relative block size on the equilibrium elastic modulus, G_e, we have performed oscillatory shear simulations for the same set of concentrations and relative midblock volumes used in the micelle bridging study. As an example of the results from our study, in Figure 8, we present oscillatory shear simulations for the $A_1B_{15}A_1$ copolymer. The storage modulus, $G'(\omega)$ of this system is expected to obey the modified Rouse theory for networked polymers,[8] where at high frequencies $G'(\omega)$ exhibits a power law decay with exponent 0.53, followed by a plateau region, corresponding to G_e at low frequencies (Fig. 8a). The slope of the $G'(\omega)$ decay corresponds to a bead-spring model with partial hydrodynamic interactions. Thus, we have observed the intermediate state between free-draining behavior (where chains move independently of each other) and hydrodynamic behavior (where frictional interactions dominate) that corresponds to 1/2 and 2/3 power laws, respectively,.[8] Because the frequency in a DPD simulation is expressed as $\frac{2\pi}{r_c}\sqrt{\frac{M_A}{RT}}$, where M_A is the molecular weight of the A-block, the decay of the storage modulus is nearly inaccessible by experiment because of too high frequency regime and, therefore, is beyond the scope of our study. Because gels are characterized by G', which are nearly independent of

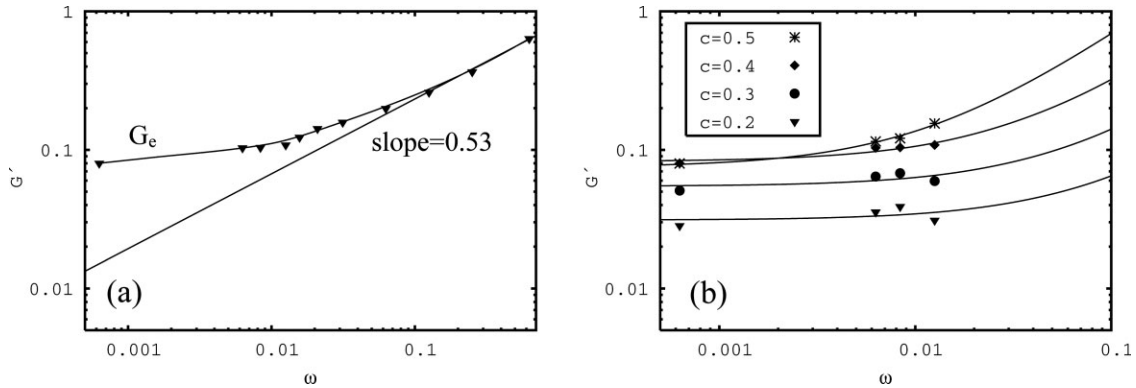

FIGURE 8 Storage modulus, G' for the $A_1B_{15}A_1$ triblock copolymer as a function of frequency, ω: (a) example of the storage modulus for concentration, $c = 0.4$ and period $p = 2\Pi/\omega$ from 10 to 10000. The solid lines are approximations using a quadratic Bezier curve representation. (b) The plateau region of the storage modulus, G' at various concentrations. Solid lines represent linear extrapolations for accessing experimental frequencies.

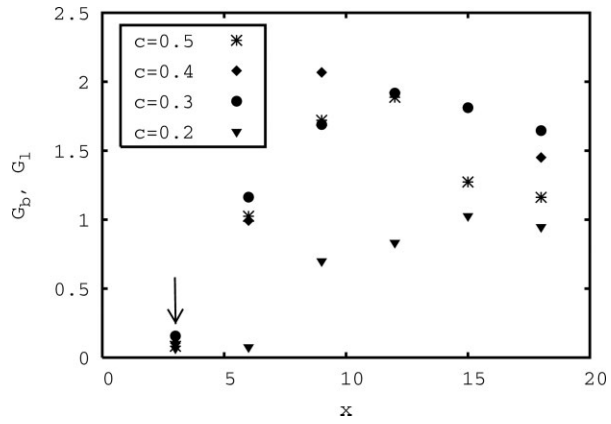

FIGURE 9 Contribution of a single bridge, G_b and loop, G_l to the equilibrium elastic modulus as a function of the relative block size, x at various volume fractions of the copolymer, c. G_b and G_l are plotted in DPD units. The arrow indicates G_l evaluated for the $A_1B_3A_1$. All other data points correspond to G_b.

ω over several orders of magnitude, we can exploit the plateau region of G' for the subsequent analysis. An example of the plateau regime of G' as a function of concentration is shown in Figure 8.

Following the procedure described earlier in Viscoelastic Property Calculations Section, we have obtained G_e for various concentrations and midblock sizes and presented our results in Figure 9. From our bridge fraction study in Bridge Fraction Section, we determined that the midblock of $A_1B_3A_1$ forms only loops; therefore, we can estimate the elastic modulus of a single loop to the elastic modulus, G_l from eq 15 by setting ϕ_b equal to 0. Assuming that G_l does not change with concentration or polymer length, we have estimated $G_l = 0.11$ (in DPD units). By using this quantity in eq 15, we have found the elastic modulus of a single bridge, G_b; results are shown in Figure 9. Because G_b is typically an order of magnitude larger than G_l, we have concluded that the contribution of the loops compared with the bridges is negligible for the unentangled polymeric gel. This finding contradicts with experimental observations that the contributions of the individual loops and tails to the equilibrium elastic modulus may become comparable with bridges.[7] The explanation of this disagreement is the following. Because of the soft potentials we have used in this study, our simulations cannot realistically describe excluded volume effects. As a result, the polymer chains can pass through each other without an effective barrier to chain crossing. This behavior leads to a diminished effect on the loop elasticity, i.e., we have found G_l to be an order of magnitude smaller than the measured experimental value.[7] For the simulation sizes used in this study, the domains do not exhibit long-range order in their spatial arrangement. This effect could also contribute to the reduction of the loop elasticity. Because of these features, we can assume that the loop contribution, G_l, does not depend on concentration nor midblock size and is therefore negligible. To account for excluded volume and entanglement effects, in future work we will improve our studies by introducing a noncrossing condition within the DPD method,[49,50] which may serve to mimic the entanglement constraints of the real systems.

From entropic elasticity theory,[8] the contribution of a single bridge to the equilibrium elastic modulus can be estimated from

$$G_b = g\frac{r_E^2}{r_0^2}k_BT, \tag{18}$$

where g is a coefficient on the order of unity, determined by a method for calculating chain entropy.[3] r_E^2 is the mean square end-to-end distance of a bridge, and r_0^2 is the mean square end-to-end distance of the same bridge, if it is not constrained by a network. (Note that k_BT is 1 for our simulation.) r_E^2 depends on the average distance between micelles and characterizes the stretching of the midblocks.[47] Our simulations have found that the average distance between micelles decreases with concentration (data are not shown). The ratio r_E^2/r_0^2 would be equal to 1 for the temperature and concentration at which a network was produced if there was no midblock stretching.[8] However, for the short midblocks and the low copolymer concentration, r_E^2/r_0^2 is expected to be higher than unity. Figure 9 reflects stretching of the midblock bridges for the majority of our data, which is consistent with $G_b > 1$. At $c = 0.2$, G_b becomes less than 1 for $x < 15$. We attribute this to syneresis that has occurred (Fig. 3a), where the "soft" solvent phase primarily determines the elastic modulus, and thus, the contribution of a single bridge is diminished. This finding is in agreement with experimental data and the conclusions of Watanabe et al.[7] G_b also decreases for $x = 18$ for the reason that these long midblocks are not considerably stretched. This effect becomes more prominent for $c = 0.5$, reflecting the average decrease of micelle spacing for higher copolymer concentration. We have used the combined variable $\mu = \mu = g(r_E^2/r_0^2)$ by averaging our data for all concentration and block sizes, excluding $G_b \geq 1 \pm 0.1$ and have found $\mu \approx 1.65$. This parameter is expected to characterize approximately the equilibrium modulus for $x = 9$ to 18.

Mapping our results to actual values of the elastic modulus for the ABA triblock copolymer, we have finally obtained the following conventional equation for the elastic modulus for unentangled gels:

$$G_e = \frac{\mu RT}{v_A(x+2)}c\phi_b(x, c, \chi_{ij}), \tag{19}$$

In eq 19, the volume fraction, c, the molar volume of the A-block, v_A, and the degree of incompatibility, χ_{ij}, characterize the physical triblock copolymer and solvent. The relative size of the midblock with respect to the endblock, x, is evaluated from eq 12. Using these parameters, the bridge fraction ϕ_b (x, c, χ_{ij}) is determined from equilibrium DPD simulation. The fit from this analysis of the equilibrium shear modulus and the simulation results are shown in Figure 10, where one can see that G_e matches well with simulation results for triblock copolymers at $c > 0.2$ with large-sized midblock

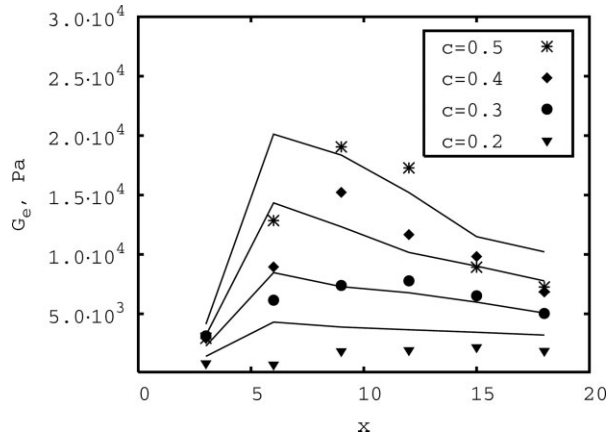

FIGURE 10 Elastic modulus, G_e for $A_1B_xA_1$ as a function of the relative block size, x at various volume fractions, c. Simulation data are represented with points and solid lines are fit to eq 19 with $\mu = 1.65$.

relative to the endblock ($x \geq 9$) if μ is equal to 1.65. Furthermore, we have found agreement with the work of Raspaùd et al. that the plateau for the elastic modulus in a selective solvent for gels in the semidilute regime made from unentangled chains is comparable to the Rouse modulus.[9]

The elastic modulus at $c < 0.2$ obtained from nonequilibrium simulation is significantly lower than its value estimated from the bridge fraction. This disagreement between results obtained from equilibrium and nonequilibrium simulations is explained by the separation of liquid from the gel at the small concentration [Fig. 3(a)]. As a consequence, we cannot predict the modulus at $c = 0.2$ from equilibrium simulation alone.

Our simulations show the elastic modulus of unentangled triblock chains with the same volume of the endblock for each concentration has a maximum value and then decreases with increasing x. The elastic modulus of unentangled polymeric gel in a strongly selective solvent seems to have a broad peak for x between 6 and 12.

Assuming the same concentration and volume of the triblock copolymer, the elastic modulus in eq 19 depends only on the bridge fraction. For the case of $\chi_{AB}M \geq 50$, ϕ_b increases with increasing relative volume of the midblock for $x < 9$ and reaches a plateau for the midblock size for $x \geq 9$, which corresponds to $f_A > 0.2$ (eq 12) for each copolymer concentration. Taking into account these findings, we predict that the maximum elastic modulus of the gel made of ABA triblock copolymers of low molecular weight in a B-block selective solvent for the particular polymer size and concentration occurs if the volume fraction of the endblock in the "dry" copolymer is less than 20%.

The main advantage of this approach (eq 19) is that it can estimate the elastic response of ABA triblock copolymers of low molecular weight in a midblock-selective solvent directly from the morphology of the gels obtained from equilibrium DPD simulations by evaluating ϕ_b (x, c, χ_{ij}). Because nonequilibrium shear simulation is not necessary, this approach greatly reduces the simulation time.

Equation 19 is valid only for block copolymers of relatively low molecular weight where entanglement does not likely occur. For copolymers with higher molecular weight, entanglements would give rise to a large additional contribution to the elastic modulus.[8]

CONCLUSIONS

The equilibrium and nonequilibrium oscillatory-shear DPD simulation methods have been used for mesoscale simulation of gel-forming ABA triblock copolymer in a midblock-selective solvent. Our results indicate that the bridge fraction, ϕ_b, increases with increasing copolymer concentration and is less significant at higher concentrations. We have demonstrated that for a strongly selective solvent and for $\chi_{AB}M > 50$, ϕ_b increases with increasing relative volume of the midblock. When the size of the midblock becomes significantly larger compared with the endblock size ($x > 9$), ϕ_b reaches a plateau in the range of 0.40 to 0.66 as the copolymer concentration increases. We have observed that the elastic response of a gel made of ABA triblock copolymers of low molecular weight in a B-block selective solvent and for $\chi_{AB}M > 50$ is comparable with the Rouse modulus. This fact allows us to estimates the absolute value of the elastic modulus of unentangled ABA triblock copolymers directly from the morphology of its micellar gel by using equilibrium DPD simulations. We have demonstrated that our simulation results are in good qualitative agreement with experimental data and theoretical predictions. Moreover, our work supports the use of DPD simulation methods to study mechanical and structural properties of various polymeric gels. The knowledge derived from the types of mesoscale simulations performed here will reduce the time and effort necessary to perform experiments, which will eventually allow us to tune the mechanical properties of ABA triblock copolymer gels for specific applications. However, to extend our approach and predict mechanical properties of triblock copolymer of high molecular weight, entanglements should be implemented in the DPD simulation,[49,50] or other simulation techniques should be exploited, such as the "Sliplink" models adopted for block copolymers.[51] We defer exploration of entangled networks made of triblock copolymers of higher molecular weight to later work.

This research was supported in part by an appointment to the Postgraduate Research Participation Program at the U.S. Army Research Laboratory (USARL) administered by the Oak Ridge Institute of Science and Education through an interagency agreement between the U.S. Department of Energy and USARL. V. Ganesan and V. Pryamitsyn acknowledge support from the U.S. Army Research Office under Grant No. W911NF-07-1-0268.

REFERENCES AND NOTES

1 Laurer, J. H.; Khan, S. A.; Spontak, R. J Langmuir 1999, 15, 7947–7955.

2 Juliano, T. F.; Forster, A. M.; Drzal, P. L.; Weerasooriya, T.; Moy, P.; VanLandingham, M. R. J Mater Res 2006, 21, 2084–2092.

3 Drozdov, A. D.; Agarwal, S.; Gupta, R. K. Int J Eng Sci 2005, 43, 304–320.

4 Tanaka, F. J Non-Cryst Solids 2002, 307, 688–697.

5 Shen, W.; Kornfield, J. A.; Tirrell, D. A. Soft Matter 2007, 3, 99–107.

6 Szczubiałka, K.; Ishikawa, K.; Morishima, Y. Langmuir 2000, 16, 2083–2092.

7 Watanabe, H.; Sato, T.; Osaki, K. Macromolecules 2000, 33, 2545–2550.

8 Ferry, J. D.; In Viscoelastic Properties of Polymers; Wiley: New York, 1980.

9 Raspaùd, E.; Lairez, D.; Adam, M.; Carton, J.-P. Macromolecule 1996, 29, 1269–1277.

10 Doi, M.; Edwards, S. F.; In The Theory of Polymer Dynamics; Oxford Science: New York, 1986.

11 Semenov, A. N.; Joanny, J.-F.; Khokhlov, A. R. Macromolecules 1995, 28, 1066–1075.

12 Bedrov, D.; Smith, G. D.; Douglas, J. F. Europhys Lett 2002, 59, 384–390.

13 Cao, X.; Xu, G.; Li, Y.; Zhang, Z. J Phys Chem A 2005, 109, 10418–10423.

14 Cass, M. J.; Heyse, D. M.; Blanchard, R.-L.; English, R. J. J. Phys Condens Matter Chem A 2008, 20, 335103

15 Groot, R. D.; Agterof, W. G. M. Macromolecules 1995, 28, 6284–6295.

16 Guo, L.; Luijten, E. J Polym Sci B 2005, 43, 959–969.

17 Khalatur, P. G.; Khokhlov, A. R.; Mologin, D. A. J Chem Phys 1998, 109, 9614–9622.

18 Khalatur, P. G.; Khokhlov, A. R.; Kovalenko, J. N.; Mologin, D. A. J Chem Phys 1999, 110, 6039–6049.

19 Zhulina, E. B.; Halperin, A. Macromolecule 1992, 25, 5730–5741.

20 Matsen, M. W.; Schick, M. Macromolecule 1994, 27, 187–192.

21 Jones, R. L.; Kane, L.; Spontak, R. J Chem Eng Sci 1996, 51, 1365–1375.

22 Kim, S. H.; Jo, W. H. Macromolecule 2001, 34, 7210–7218.

23 Karatasos, K.; Anastasiadis, S. H.; Pakula, T.; Watanabe, H. Macromolecules 2000, 33, 523–541.

24 Nguyen-Misra, M.; Mattice, W. L. Macromolecules 1995, 28, 1444–1457.

25 Watanabe, H.; Sato, T.; Osaki, K.; Yao, M.-L.; Yamagishi, A. Macromolecules 1997, 30, 5877–5892.

26 Takano, A.; Kamaya, I.; Takahashi, Y.; Matsushita, Y. Macromolecule 2005, 38, 9718–9723.

27 Hoogerbrugge, P.; J; Koelman, J. M. V. A. Europhys Lett 1992, 9, 155–160.

28 Koelman, J. M. V. A.; Hoogerbrugge, P. J. Europhys Lett 1993, 21, 363–368.

29 Español, P.; Warren, P. B. Europhys Lett 1995, 30, 191–196.

30 Groot, R. D.; Madden, T. J. J Chem Phys 1998, 108, 8713–8724.

31 Groot, R. D.; Rabone, K. L. Biophys J 2001, 81, 725–736.

32 Spenley, N. A. Europhys Lett 2000, 49, 534–540.

33 Allen, M. P.; Tildesley, D. J.; In Computer Simulation of Liquids; Oxford University Press: New York, 1987.

34 Pryamitsyn, V.; Ganesan, V. Macromolecule 2006, 39, 844–856.

35 Lees, A. W.; Edwards, S. F. Solid State Phys 1972, 5, 1921–1929.

36 Underhill, P. T.; Doyle, P. S. J Non-Newtonian Fluid Mech 2004, 122, 3–31.

37 Groot, R. D.; Warren, P. B. J Chem Phys 1997, 107, 4423–4435.

38 Trofimov, S. Y. Thermodynamic Consistency in Dissipative Particle Dynamics. Ph.D. Thesis; Eindhoven University of Technology: The Netherlands, 2003.

39 Pivkin, I. V.; Karniadakis, G. E. J Chem Phys 2006, 124, 184101-184101-7.

40 Nakamura, H.; Tamura, Y. J Plasma Phys 2006, 72, 1001–1004.

41 Venturoli, M.; Smit, B.; Sperotto, M. M. Biophys J 2005, 88, 1778–1798.

42 Amelar, S.; Eastman, C. E.; Morris, R. L.; Smeltzly, M. A.; Lodge, T. P.; von Meerwall, E. D. Macromolecules 1991, 24, 3505–3516.

43 Ding, Y.; Sokolov, A. P. J Polym Sci Part B: Polym Phys 2004, 42, 3505–3511.

44 Lai, C.; Russel, W. B.; Register, R. A. Macromolecule 2002, 35, 841–849.

45 Bernardo, G.; Vesely, D. J Appl Polym Sci 2008, 110, 2393–2398.

46 Fetters, L. J.; Lohse, D. J.; Colby, R. H. In Physical Properties of Polymers Handbook; Mark, J. E., Ed.; A. I. P. Press: Woodbury, NY, 1996.

47 Seitz, M. E.; Burghardt, W. R.; Faber, K. T.; Shull, K. R. Macromolecule 2007, 40, 1218–1226.

48 Vega, D. A.; Sebastian, J. M.; Loo, Y.-L.; Register, R. A. J Polym Sci Part B: Polym Phys 2001, 39, 2183–2197.

49 Goujon, F.; Malfreyt, P.; Tildesley, D. J. J Chem Phys 2008, 129, 034902-034902-9

50 Lahmar, F.; Rousseau, B. Polymer 2007, 48, 3584–3592.

51 Masubuchi, Y.; Iannirubertо, G.; Greco, F.; Marrucci, G. J Non-Cryst Solids 2006, 352, 5001–5007.